

# APPENDIX B

N 9 3 - 1 5 5 9 1

## A Liquid Xenon Imaging Telescope for Gamma-Ray Astrophysics: Design and Expected Performance

E. Aprile, R. Mukherjee, D. Chen and A. Bolotnikov  
Physics Department and  
Columbia Astrophysics Laboratory, Columbia University  
538 West 120th Street, New York, NY 10027, USA

Presented at the: 3<sup>rd</sup> *International Conference on Advanced Technology and  
Particle Physics*, Como, Italy, 22 – 26 June, 1992  
To be published in: *Nuclear Physics B (Proc. Suppl.)*

COLUMBIA UNIVERSITY  
DEPARTMENTS OF  
PHYSICS and ASTRONOMY  
NEW YORK, NEW YORK 10027

# A Liquid Xenon Imaging Telescope for Gamma-Ray Astrophysics: Design and Expected Performance

E. Aprile, R. Mukherjee, D. Chen, and A. Bolotnikov

Physics Department and Columbia Astrophysics Laboratory  
Columbia University, New York, NY 10027

A high resolution telescope for imaging cosmic  $\gamma$ -ray sources in the MeV region, with an angular resolution better than  $0.5^\circ$  is being developed as balloon-borne payload. The instrument consists of a 3-D liquid xenon TPC as  $\gamma$ -ray detector, coupled with a coded aperture at a distance of 1 meter. A study of the actual source distribution of the 1.809 MeV line from the decay of  $^{26}\text{Al}$  and the 511 keV positron-electron annihilation line is among the scientific objectives, along with a search for new  $\gamma$ -ray sources. The telescope design parameters and expected minimum flux sensitivity to line and continuum radiation are presented. The unique capability of the LXe-TPC as a Compton Polarimeter is also discussed.

## 1. INTRODUCTION

Gamma-ray telescopes with true imaging capability and high flux sensitivity are essential for studying the highest-energy phenomena in the universe. Fine imaging provides accurate positioning of the sources detected within the FOV and good angular resolution to map regions of diffuse emission and separate point source contributions. The importance of true source imaging is particularly evident in the study of two of the most pressing problems in low energy  $\gamma$ -ray astronomy: the 1.089 MeV line emission from the decay of  $^{26}\text{Al}$  and the 511 keV positron-electron annihilation line emission from the Galactic Center.

In 1977, Ramaty and Lingenfelter [1] suggested that galactic nucleosynthetic production of  $^{26}\text{Al}$  in supernova events over the past few million years could give rise to a detectable  $\gamma$ -ray line at 1.809 MeV. This line arises from the electron capture (18%) or positron decay (82%) of the million-year mean life  $^{26}\text{Al}$  and was first detected in 1984 [2] at a flux level of  $4.3 \pm 0.8 \times 10^{-4}$  photons  $\text{cm}^{-2} \text{s}^{-1} \text{rad}^{-1}$  at the Galactic Center. Several subsequent confirmations of the line energy and flux level have been made. Some potential sources of  $^{26}\text{Al}$ , which have been proposed, are supernovae, novae, red giants in the Asymptotic

Giant Branch (AGB), Wolf-Rayet stars or nearby OB stars (see e.g., [3] for a recent review). Since these objects have more or less known or inferred galactic distributions, it is believed that a measurement of the spatial distribution of the  $^{26}\text{Al}$  1.809 MeV line intensity will identify the  $^{26}\text{Al}$  source. The only instrument which could measure this radiation with imaging capability, is the Compton telescope, the most advanced version of which is COMPTEL on the *COMPTON* Observatory. COMPTEL however cannot directly measure the 1.809 MeV spatial distribution. The only definite statement that can be made about the  $^{26}\text{Al}$  spatial distribution from the latest COMPTEL results, at the present time, is that a point source near the Galactic Center can be excluded [4]. Clearly, there is a requirement to measure directly the spatial distribution of the 1.809 MeV line with a true imaging telescope.

As for the 511 keV line, the debate between point like and diffuse nature of the emission continues to date and can only be fully resolved with a high level imaging map of the Galactic Center region at  $\gamma$ -ray energies.

At the present time the OSSE instrument on the *COMPTON* Observatory is mapping the distribution of the annihilation line [5]. Since the OSSE measurements give the lowest galactic center flux measurements so far Skibo, Ramaty and Leventhal [6] have used these results

and other off-center measurements to test different models for the origin of the diffuse or steady galactic plane 511 keV component. On the other hand, the origin of the variable narrow line galactic 511 keV radiation may be associated with the bright hard X-ray source 1E1740.7-2942 which was studied by the imaging telescope SIGMA on the *GRANAT* satellite during the spring-fall of 1990 and in early 1991. Sunyaev *et al.* [7] have identified three spectral states for this source which range from a "low state," a normal (Cygnus X-1 like) state to a hard state in which a bump appears in the spectrum between (300–600) keV. The broad feature of the spectrum has been interpreted as annihilation of positrons in a hot medium ( $\sim 40$  keV). This is consistent with the temperature of the accretion disk derived from the X-ray continuum spectrum.

Subsequently it was proposed [8,9] that in addition this high energy source injects positrons into a molecular cloud where they slow down and annihilate to produce the narrow component of the 511 keV line emission.

Future studies of the 511 keV emission require the most advanced imaging telescope with good to excellent energy resolution.

Of the techniques proposed for  $\gamma$ -ray imaging and spectroscopy of astrophysical sources, the Liquid Xenon Time Projection Chamber (LXe-TPC) is among the most promising. The properties of liquid xenon make it very efficient for  $\gamma$ -ray detection. When used in an ionization chamber, operated in the time projection mode, this medium offers a combination of high detection efficiency, excellent spatial resolution and very good energy resolution. Like an electronic bubble chamber, a LXe-TPC with three-dimensional position sensitivity is capable of visualizing the complex histories of  $\gamma$ -ray events initiated by either Compton scattering or pair-production. As a result, efficient background rejection is also achieved, reducing the requirement for massive anticoincidence shielding of the type that is required for germanium or sodium iodide  $\gamma$ -ray detectors. The angular resolution of the LXe-TPC as a Compton telescope is however limited, in the few MeV region, by the small separation between two successive  $\gamma$ -ray interactions [13]. To achieve

imaging with good angular resolution at low energies, the combination of the imaging LXe-TPC with a coded aperture is proposed.

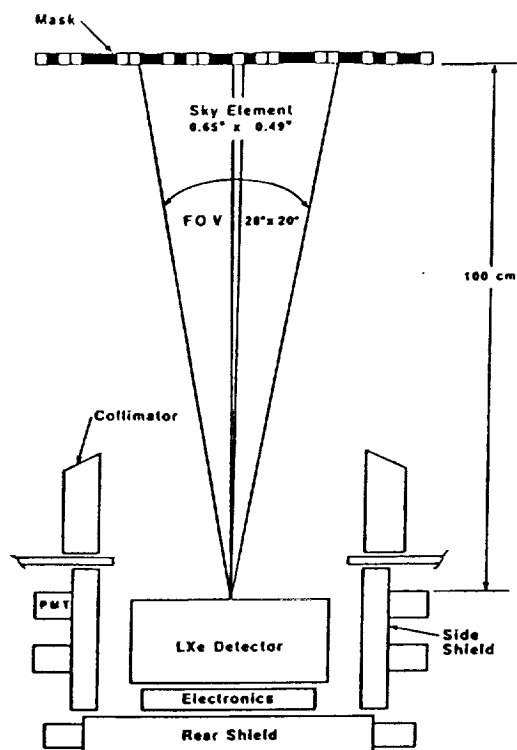
A unique consequence of the LXe-TPC imaging capability is its sensitivity as a Compton polarimeter. Besides the precise determination of the energy and incident direction of a photon, determination of its polarization state can give further information on the source of  $\gamma$  rays. The main production mechanisms which can give polarized  $\gamma$  rays are: bremsstrahlung from electron beams, electron synchrotron radiation, electron curvature radiation, and  $\gamma$  rays from de-excitation of nuclei excited by directed ion beams. In the case of the Crab Nebula it has been determined that the nebular X-ray emission is polarized [10]. Existence of UHE ( $> 10^{14}$ ) electrons in this source could yield polarized nebular  $\gamma$ -rays of a few MeV. If curvature radiation from electrons is the source of MeV  $\gamma$  rays in pulsars, such as the Crab and Vela, then polarization might also be expected.

In general it has been recognized in the study of X-ray sources, that measurement of the direction and magnitude of the photon polarization could significantly contribute to a better understanding of the physical processes in compact objects, such as pulsars, Black Holes and AGN.

## 2. TELESCOPE DESIGN

### 2.1. Introduction

The telescope is schematically shown in Fig. 1. It consists of a coded aperture mask, located 1 meter above a LXe-TPC. The sensitive area of the TPC is  $39 \times 28$  cm<sup>2</sup>. The active depth of liquid xenon is 10 cm. Fig. 2 shows the LXe-TPC in more detail. The event trigger to the readout electronics is provided by the fast primary scintillation light detected by two UV sensitive PMTs. The intrinsic instrumental angular resolution in the coded mask configuration is determined by the size of the mask unit cell, the mask-detector separation, and by the accuracy to which the photon interaction points in the detection plane can be determined. The coded mask that we have assumed in our design and Monte Carlo simulations consists of a  $85 \times 83$  element pattern of



Energy Range	0.3-10 MeV
Energy Resolution	4.5% FWHM at 1 MeV
Spatial resolution	1 mm
Geometrical area	1200 cm <sup>2</sup>
FOV (Fully Coded)	28° x 20° FWHM
Angular resolution	30'
Point source location accuracy	1' (10 $\sigma$ source)
Min Flux (Line)	$8 \times 10^{-5}$ ph cm <sup>-2</sup> s <sup>-1</sup>
3 $\sigma$ at 1 MeV	( $3 \times 10^4$ s)
Min Flux (Continuum)	$3 \times 10^{-7}$ ph cm <sup>-2</sup> s <sup>-1</sup> keV <sup>-1</sup>
3 $\sigma$ at 1 MeV	( $3 \times 10^4$ s)

Fig. 1. Schematic of the LXe-TPC/coded mask imaging  $\gamma$ -ray telescope.

$0.91 \times 0.58 \times 1.2$  cm<sup>3</sup> thick blocks of tungsten alloy. The 1 meter separation between the mask and the LXe detector plane is determined by the University of New Hampshire gondola [11] which we plan to use for the first balloon flight. This defines a pixel element of angular dimension  $0.65^\circ \times 0.49^\circ$ . The nominal FOV is  $28^\circ \times 20^\circ$

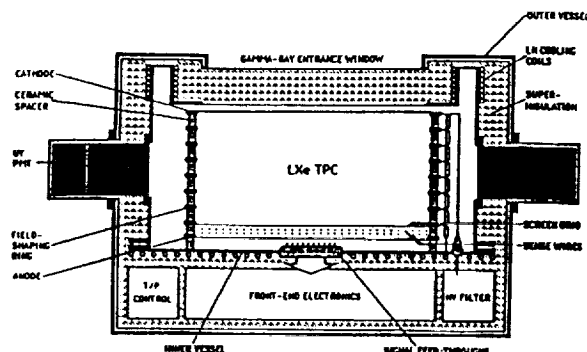


Fig. 2. Schematic of the LXe-TPC detector.

and the source localization accuracy is estimated to be  $\sim 1$  arcminute, for a  $10\sigma$  source strength. For background suppression at balloon altitude an active shield has been assumed around the detector. The type and amount of shield needed will ultimately be determined by the type of event triggering and selection on board, by dead time consideration, telemetry rate as well as cost and weight consideration.

## 2.2. The LXe-TPC: Status of Development

A LXe-TPC works on the principle that free ionization electrons liberated by a charged particle in the liquid can drift, under a uniform electric field, from their point of creation towards a signal read-out region. Here the charge signals induced or collected on sensing electrodes are detected to yield both the spatial distribution of the ionizing event and its energy.

For  $\gamma$ -rays it is the electrons or positrons created by photoabsorption, Compton scattering or pair production, which will ionize as well as excite the xenon atoms creating a large number of electron-ion pairs and scintillation photons. For 3-D imaging of  $\gamma$ -ray events in LXe we plan to use a sensing electrodes geometry based on the original design by Gatti *et al.* [12]. Two orthogonal induction wire planes separated from the drift region by a screening grid, give the X-Y event information. The measured drift time, referred to the scintillation trigger, and the known drift velocity provides the Z-information. The total event energy is measured from the total charge collected on an anode plate, placed below the induction

wires.

In order to verify the feasibility of such a detector, the Columbia group started in 1989 an intensive R&D program on LXe. The attenuation length of electrons and UV photons in purified liquid xenon, the ionization and scintillations yields of electrons and alpha particles, the energy and spatial resolution have been studied.

The experimental results obtained on these aspects relevant for the development of a liquid ionization TPC, are documented in several references [13-18]. Especially relevant are the latest experimental results obtained with a 3.5 liter 2D-TPC prototype [19] equipped with a multi-wire structure to detect the induction signals in liquid xenon. The results demonstrate both the capability of a large volume LXe detector to provide similar or better energy resolution than the previously reported value of 4.5% FWHM for 1 MeV radiation, as well as the imaging capability.

Figure 3 shows an example of collection and induction signals produced by a  $\gamma$ -ray event in the LXe-TPC prototype. The induction signal, which has the expected triangular shape, has a large S/N ratio of 12:1, even for a typical point-like charge deposition produced by a  $\gamma$ -ray interaction. The dependence of the induced signal on the lateral position of the drifting electron cloud

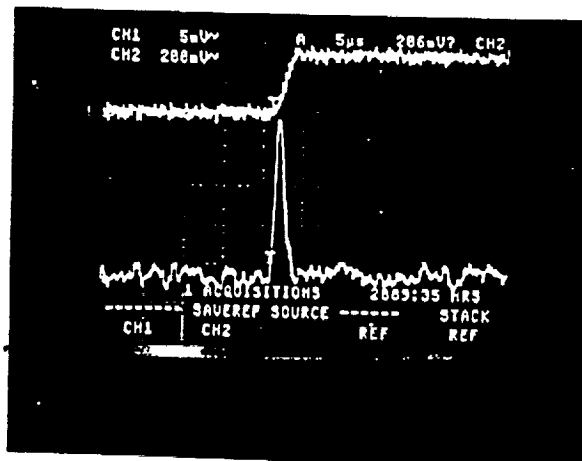


Fig. 3. Collection signal (upper trace Gain=1) and induction signal (lower trace Gain=400) produced by a  $\gamma$ -ray event in the 3.5 liter LXe-TPC prototype.

with respect to the wire cell [19], offers the possibility to derive the spatial coordinate of each event by weighting the signal amplitude on neighbouring wires. Thus the spatial resolution in the X-Y plane, can be better than  $s/\sqrt{12}$ , where  $s$  is the wire spacing.

Experimental work on the operation and performance of the LXe TPC prototype implemented for full 3-D imaging and triggered by the scintillation light is in progress.

### 3. TELESCOPE PERFORMANCE: MONTE CARLO RESULTS

#### 3.1. Background Rate and Minimum Flux Sensitivity.

To calculate the background expected in the LXe-TPC/coded mask telescope at balloon altitudes, we have taken into account the dominant atmospheric and cosmic diffuse components, entering the forward aperture of the telescope or leaking through the active shield (5 cm thick CsI). The flux and angular distribution of the atmospheric  $\gamma$ -rays used in the calculation were taken from the parameterized forms given by Costa *et al.* [20] and the cosmic diffuse spectrum used was that given by Shoñfelder, Graser and Daugherty [21]. The internal backgrounds from natural radioactivity, cosmic ray induced radioactivity and activation of instrument materials have been neglected, as the majority of these single site events can be rejected by simple fiducial volume cuts.

The results of the calculation are shown in Fig. 4. The integrated flux over the 0.1-10 MeV region gives about 340 counts/sec, consistent with typical background rates measured at the assumed altitude. An event reconstruction algorithm based on the kinematics of Compton scattering was developed and used for identification and rejection of background events [22]. As shown in Fig. 4, a background reduction of approximately a factor of 10 is obtained by identifying  $\gamma$ -rays which kinematically couldn't have come through the FOV of the telescope, and by applying a fiducial volume cut to remove low energy events.

Based on the calculated  $\gamma$ -ray detection efficiency [22] and the calculated background rate,

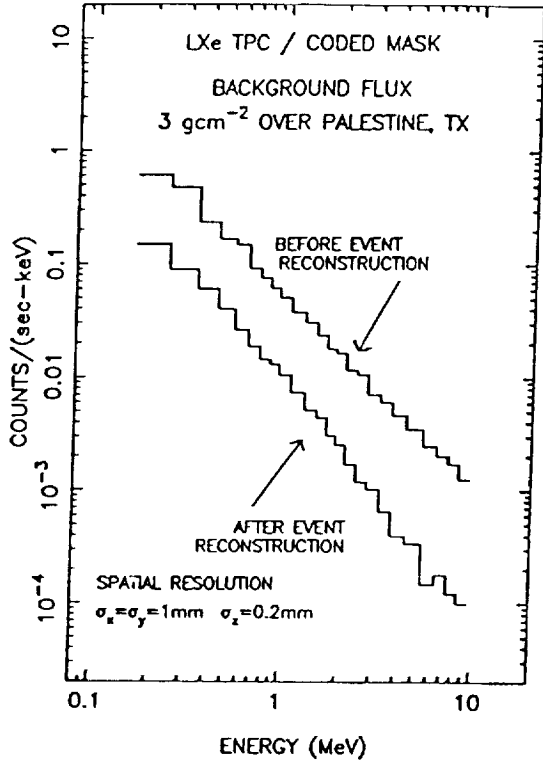


Fig. 4. Monte Carlo calculation of the background flux at balloon altitude.

we have obtained the  $3\sigma$  minimum flux sensitivity shown in Fig. 5. With a typical balloon flight exposure of  $3 \times 10^4$  s, the  $3\sigma$  line sensitivity is  $6 \times 10^{-5}$  photons  $\text{cm}^{-2} \text{s}^{-1}$  (1.8 MeV line) and  $9 \times 10^{-5}$  photons  $\text{cm}^{-2} \text{s}^{-1}$  (511 keV line). The continuum sensitivity is  $3 \times 10^{-7}$  photons  $\text{cm}^{-2} \text{s}^{-1} \text{keV}^{-1}$  at 1 MeV. The sensitivity curves of the instruments, shown for comparison, have been taken from Winkler [23]. When combined with the excellent source localization accuracy, the high sensitivity of the LXe-TPC telescope makes it competitive with many satellite instruments, even with the much shorter observation time available in a balloon flight.

### 3.2. Simulated Observations of the Crab and 511 keV Line

The Crab Nebula/Pulsar will be the primary target for the first verification balloon flight of the LXe-TPC coded mask  $\gamma$ -ray telescope. This source is one of the most intense in our energy

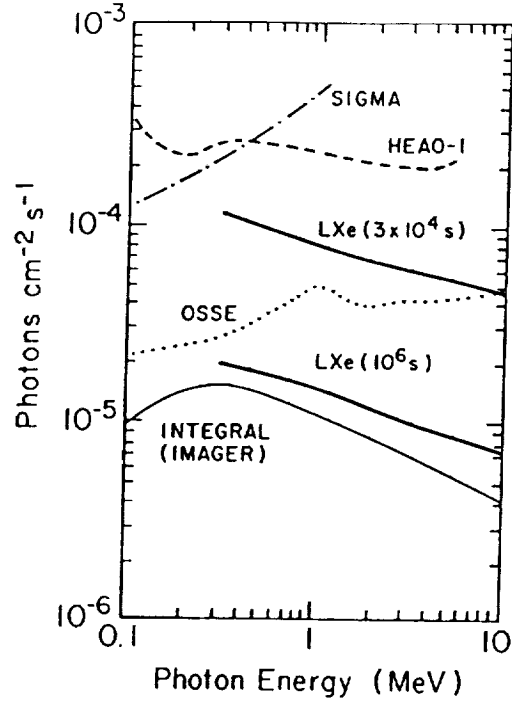


Fig. 5.  $3\sigma$  minimum line flux sensitivity of the LXe-TPC/coded mask  $\gamma$ -ray telescope.

range and is stable, both in intensity and spectrum. Monte Carlo simulations of the expected Crab signal were performed using the complete telescope system shown in Fig. 1.

The Crab Nebula was assumed to be a point source in the sky with a spectrum equal to  $5.5 \times 10^{-4} (E/100 \text{ keV})^{-2.2}$  photons  $\text{cm}^{-2} \text{s}^{-1} \text{keV}^{-1}$  at 10 MeV [24]. The source was aligned with the telescope axis and the observing time was  $10^4$  s. The estimated background of Fig. 4, after event reconstruction, was uniformly distributed in the detector's plane and added to the shadowgram of the source. Figure 6 shows the resulting deconvolved image of the Crab, for the energy interval 0.3 – 0.5 MeV. The Crab signal dominates over the background up to several MeV with a S/N of about  $20\sigma$ .

Simulated observations have also been performed for the low and high state of the 511 keV Galactic Center annihilation line. A  $10^4$  s exposure time was assumed. The source was placed in the center of the FOV, and superimposed on

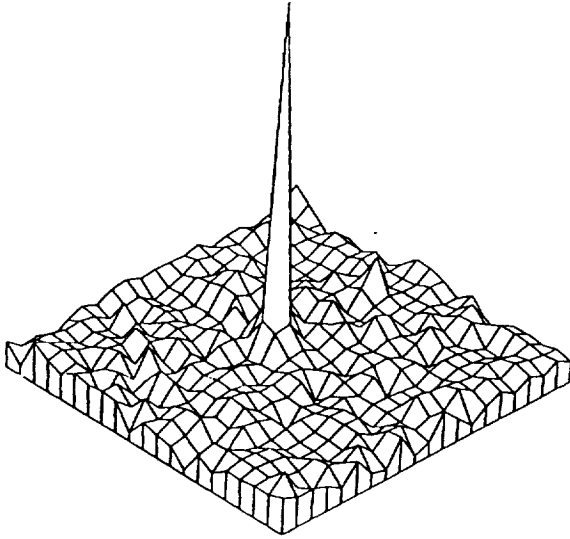


Fig. 6. Monte Carlo simulation of the Crab as a point  $\gamma$ -ray source in the energy range (0.3–0.5 MeV).

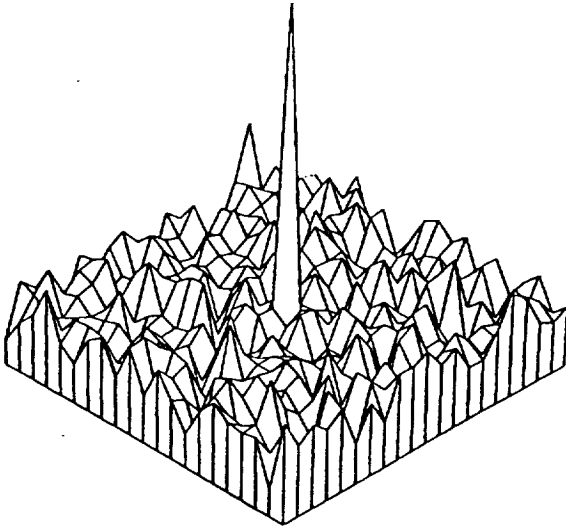


Fig. 7. Monte Carlo simulation of the 511 keV Galactic Center point source observed for High State.

a uniformly distributed background of  $4 \times 10^{-2}$  counts  $s^{-1} \text{ keV}^{-1}$ , as from our estimate. The intensity of the 511 keV line source was chosen to be  $2 \times 10^{-4}$  photons  $\text{cm}^{-2} \text{ s}^{-1}$  for the “low state” and  $1 \times 10^{-3}$  photons  $\text{cm}^{-2} \text{ s}^{-1}$  for the “high state”.

Figure 7 shows the result of the 511 keV image for the “high state”. Even in the “low state”, the 511 keV flux can be detected by our instrument at a satisfactory significance level of  $\sim 4\sigma$ .

### 3.3. Polarization Sensitivity

The LXe-TPC imaging capability is also ideal to measure the linear polarization of the incident  $\gamma$ -ray undergoing Compton scattering. The linear polarization of  $\gamma$ -rays can be measured based on the principle that the Compton scattering process is sensitive to the polarization of the incident  $\gamma$ -ray, the cross-section for Compton scattering being the largest for the case when the direction of the scattered  $\gamma$ -ray is normal to the polarization vector of the incident  $\gamma$ -ray. The advantage of a LXe-TPC Compton Polarimeter over the conventional NaI(Tl), CsI(Tl) or Ge(Li) double scatter Compton telescopes is the enhanced detection efficiency offered by a single detector working both as scatterer and absorber, as well as its combination of good energy and position sensitivity.

A Monte Carlo program was developed to estimate the polarization sensitivity of the LXe-TPC for a 100% polarized  $\gamma$ -ray beam of energy varying from 300 keV to 4 MeV, incident normally on the detector surface. Figure 8 shows the result. For comparison, the polarization sen-

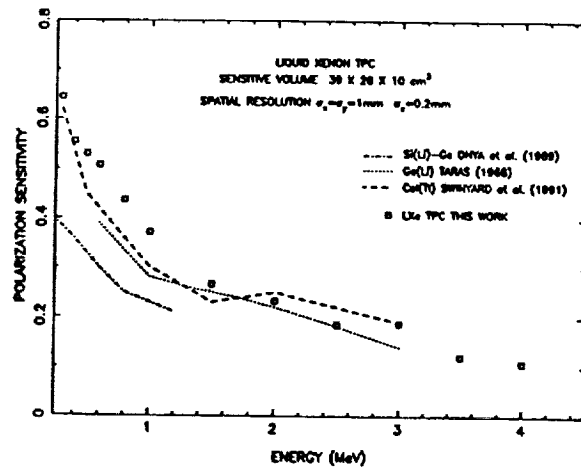


Fig. 8. Monte Carlo calculation of the LXe-TPC polarization sensitivity.

sitivity of the Ge(Li) polarimeter [25], the Si(Li) [26] and the CsI(Tl) polarimeter of the Imager on INTEGRAL [27] are also shown. The unique feature of the LXe-TPC is its capability to infer the scattering angle  $\theta$  and the azimuthal angle  $\phi$ , with an accuracy of about  $0.5^\circ$  [13], for each scattered  $\gamma$ -ray. We can thus obtain the azimuthal angular distribution of the scattered  $\gamma$ -rays by selecting events from different intervals of scattering angle. By applying the detector's response function, calculated or measured during calibration tests with polarized beams, we can deconvolute the original  $\gamma$ -ray polarization. Figure 9 shows the modulation curve in the range  $\phi = 0^\circ$  to  $\phi = 90^\circ$ , simulated for 100% polarized  $\gamma$ -rays of energy 500 keV.

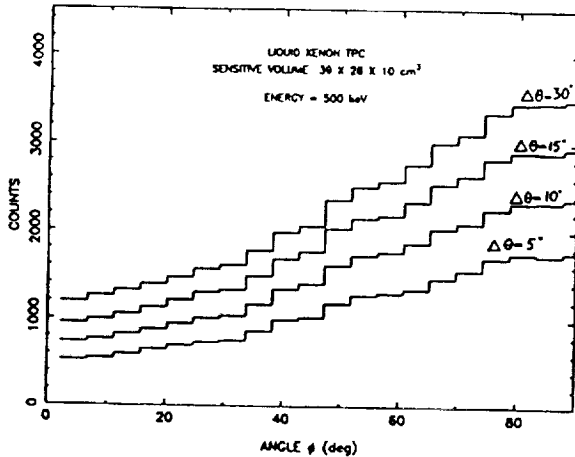


Fig. 9. Modulation curve of the LXe-TPC for 100% polarized  $\gamma$ -rays of energy 500 keV.

#### 4. CONCLUSION

The design and expected performance of a  $\gamma$ -ray imaging telescope tailored to the 0.3–10 MeV energy region have been discussed. The telescope combines the excellent properties of a liquid xenon TPC as 3-D position sensitive  $\gamma$ -ray detector with the well established imaging properties of a coded aperture mask, to achieve high efficiency, good spectroscopy and angular resolution over the entire energy range of interest. The high sensitivity to MeV  $\gamma$ -ray lines and continuum complemented with the good imaging capa-

bility will permit the observation of a variety of astrophysical sources. Important contributions to the field of low energy astrophysics as well as new discoveries are expected even in the maiden balloon flight which is planned for the end of 1994.

This work was supported by NASA (Award NAGW 2013).

#### 5. REFERENCES

- [1] R. Ramaty, and R.E. Lingenfelter, *Ap.J. (Letters)*, **213**, L5 (1977).
- [2] W.A. Mahoney *et al.*, *Ap.J.*, **286**, 578 (1984).
- [3] N. Prantzos, *Astron. Astrophys. Suppl.*, in press (1992).
- [4] R. Diehl *et al.*, *Astron. Astrophys. Suppl.*, in press (1992).
- [5] W.A. Purcell, *et al.* in *The Compton Observatory Science Workshop*, NASA Conf. Publ. 3137, eds. C.R. Shrader, N. Gehrels and B. Dennis, 43 (1992).
- [6] J.G. Skibo, R. Ramaty, M. and Leventhal, *Ap.J.*, in press (1992).
- [7] R. Sunyaev, *et al.*, *Ap. J. (Letters)*, **383**, L49 (1991).
- [8] J. Bally and M. Leventhal, *Nature*, **353**, 234 (1991).
- [9] I.F. Mirabel *et al.*, *Nature*, **358**, 215 (1992).
- [10] M.C. Weisskopf *et al.*, *Ap.J. (Letters)*, **220**, L117 (1978).
- [11] P.P. Dunphy *et al.*, *Nucl. Instr. and Meth.*, **A274**, 362 (1989).
- [12] E. Gatti *et al.*, *Trans. Nucl. Sci.*, **NS-26**, 2910 (1970).
- [13] E. Aprile, R. Mukherjee, and M. Suzuki, "EUV, X-Ray and Gamma-Ray Instrumentation for Astronomy and Atomic Physics," *SPIE Conference Proceedings*, ed. C.J. Hayley and O.H.W. Siegmund, **1159**, 295 (1989).
- [14] E. Aprile, R. Mukherjee, and M. Suzuki, *IEEE Trans. Nucl. Sci.*, **NS-37**, No. 2, 553 (1990).
- [15] E. Aprile, R. Mukherjee, R. and M. Suzuki, *Nucl. Instr. and Meth.*, **A302**, 177 (1991).
- [16] E. Aprile, R. Mukherjee, and M. Suzuki, *Nucl. Instr. and Meth.*, **A300**, 343 (1991).

- [17] E. Aprile, R. Mukherjee, and M. Suzuki, *Nucl. Instr. and Meth.*, **A302**, 177 (1991)
- [18] E. Aprile *et al.*, *Nucl. Instr. and Meth.*, **A316**, 29 (1992).
- [19] E. Aprile *et al.*, accepted for publication in *SPIE proceedings* (1992).
- [20] E. Costa, *et al.*, *Astrophysics and Space Science*, **100**, 165 (1984).
- [21] V. Schönfelder, V. Graser, V. and J. Daugherty, *Ap.J.*, **217**, 306 (1977).
- [22] E. Aprile *et al.*, accepted for publication in *Nucl. Instr. and Meth.* (1992).
- [23] C. Winkler, *Gamma-Ray Line Astrophysics*, *AIP Conf. Proc.*, **232**, p. 483 (1991).
- [24] J.C. Ling, and C.D. Dermer, *B.A.A.S.*, **22**, 1271 (1990).
- [25] P. Taras, *Nucl. Instr. and Meth.*, **61**, 321 (1968).
- [26] S. Ohya *et al.*, *Nucl. Instr. and Meth.*, **A276**, 223 (1989).
- [27] B.M. Swinyard *et al.*, *SPIE*, Vol. 1548 *Production and Analysis of Polarized X-rays*, 94 (1992).